The Urbach Rule for the Sodium- and Potassium-Halides

Tetsuhiko Tomiki, Takeo Miyata, and Hirokazu Tsukamoto

Matsushita Research Institute Tokyo, Inc., Ikuta, Kawasaki, Japan

(Z. Naturforsch. **29 a**, 145–157 [1974]; received January 2, 1973)

Phenomenological and physical aspects of the intrinsic tail spectra of the alkalihalides are studied referring to the new results on the intrinsic tail spectra of KBr and KI and to the temperature dependences of the lowest-energy Γ-exciton peak of the sodium- and potassium-halides. Systematically analysing the temperature dependence of the steepness parameter $\sigma_s(T)$ of the Urbach rule for these halides, it is found that the frequency factor has the value nearly equal to the acoustic phonon energy at X or L of each host lattice and the steepness constant σ_{s0} becomes larger in passing from fluoride to iodide. This halogen dependence of σ_{s0} is discussed in terms of the hole band-mass of the Γ_8^--level.

§ 1. Introduction

The main purpose of this work is to determine the Urbach-rule parameters for all the sodium- and potassium-halides except for KF and to find thereby the features characteristic of the intrinsic tail spectra of these halides. Since the tail spectra of intrinsic exciton lines [1, 2] as well as of impurity-induced exciton lines [1, 3] equally obey the Urbach rule, the fact alone that a given tail obeys the Urbach rule does not always constitute in itself a criterion with which the tail can be judged intrinsic or extrinsic. Therefore, it is thought worthwhile to clarify from a phenomenological point of view the concept which is meant by "intrinsic tail".

For this purpose, the present work deals with the determination of the tail spectra of KBr and KI (§ 2) and also with the thermal shift of the lowest-energy Γ-exciton peak (§ 3). The former measurement yields two important consequences:

(i) The earlier data at low temperatures of these two salts [4, 5] are to be corrected;

(ii) a comparison of these new and old data enables the specimen-temperature in a series of our works [1, 2, 6–9] to be determined with reasonable accuracy.

On the other side, the phonon dispersion curves were measured on KCl [10, 11] and NaCl [12, 13] shortly after the publication of our works on KCl [1, 6, 7] and NaCl [2, 8]. In addition to the phonon dispersion curves of the sodium- and potassium-halide lattices, there has also been an increasing compilation in the past ten years of the data concerning the temperature dependences of lattice dynamical quantities such as specific heat, elastic stiffness parameters, linear coefficients of thermal expansion, etc. With the use of these new material constants, evaluations are made on the parameters of the Urbach rule (§ 2) and of the peak-shift formulae (§ 3) in terms of the specimen-temperature for the sodium- and potassium-halides. The results thus obtained have provided the necessary data for our purpose just mentioned in the beginning.

In § 4, an empirical criterion with which the intrinsic tails can be discriminated is first proposed referring to the data on NaCl and the potassium-halides. Second, the halogen dependence of the steepness constants for the Urbach rule found in the potassium-halides (KCl, KBr, and KI) is interpreted in the framework of the theory of Toyozawa and co-workers [14–16].

Reprint requests to Dr. T. Tomiki, Matsushita Research Institute Tokyo, Inc., Othani 4896, Ikuta, Kawasaki.

§ 2. The Intrinsic Absorption Spectra in the Tail Region of Sodium- and Potassium-Halides

Detailed descriptions have already been given in preceding reports [2, 6, 17] on the equipment used in the absorption and reflection measurements and on the procedures of processing the data; hence, the exposition on these topics is omitted here.

The temperature- and energy-dependences of the absorption constant $A(E,T)$ of alkalihalide single crystals in their tail region were studied first on KBr by Martienssen [4] and subsequently on KI by Haupt [5]. According to their investigations, $A(E,T)$ can be written by the relation

$$A(E,T) = A_0 \exp\{-\sigma_s(T)\,(E_0 - E)/kT\}\,. \qquad (2.1)$$

The temperature dependence of the steepness parameter $\sigma_s(T)$ thereafter studied both theoretically [18] and experimentally [1–3] is found to be expressible as

$$\sigma_s(T) = \sigma_{s0}\frac{2kT}{\hbar\omega}\tanh\frac{\hbar\omega}{2kT}\,. \qquad (2.2)$$

Here, the steepness constant σ_{s0} is a temperature independent quantity and $\hbar\omega$ stands for effective phonon energy. A pair of Eqs. (2.1) and (2.2) will be called the Urbach rule specifically in this paper.

The single crystals of KBr and KI used in this work were purchased from Harshaw Chem. Co., USA. The absorption spectra in their tail region are presented in Fig. 1 by the thick curves through the data, open and filled circles; the spectral portion displaying an exponential dependence against photon energy E corresponds to the intrinsic tail spectra and the remainder to the spectra due to impurities. The former can be extrapolated as traced by thin lines to one convergence point whose coordinates (A_0, E_0) are given in Table 1. The temperature for each of the tail spectra is specified with the numerical value in parentheses along with the numeral alone. The former denotes the temperature read from the data of Martienssen or Haupt, and the latter is the temperature (at the specimen-holder, see below) in the present experiment. They differ from each other except in the intermediate temperature range $\sim 200\,\mathrm{K} \lesssim T \lesssim \sim 300\,\mathrm{K}$:

At the higher temperatures, the relation

$$T_c = T - 0.1\,(T - 273) \quad \text{for} \quad T \gtrsim 370\,\mathrm{K} \qquad (2.3)$$

is obtained by denoting the temperatures measured by us and by Martienssen or Haupt as T and T_c, respectively. It is conceived that the specimen temperature is closer to T_c than T, if one takes account of the experimental arrangements at high temperatures in the earlier [4, 5] and present works: our specimens heated by conduction through the specimen-holder, to which a thermocouple is fixed, were placed inside a radiation-shield cylinder cooled with liquid nitrogen. Since our temperature value T is related to the specimen-holder as mentioned in preceding reports [1, 2, 6–9], reevaluations have been made in this paper on the quantity $\sigma_s(T)$ and on the peak-shift for chlorides.

On the other hand, in the lower temperature region the tail measured by Haupt at 20 K, the broken line, is located in the lower energy region of our absorption tail at 65 K, the filled circles, identified with impurity absorptions. This observation strongly suggests that Haupt's specimens were not really cooled down to 20 K as reported, provided that the spectra are free from impurity-induced absorption. The specimen temperature is hence conceived to be closer to our temperature below 300 K. Therefore, our temperature T is adopted in this paper as the specimen temperature except in the region $T \gtrsim 370$ K where it is to be replaced by T_c according to Equation (2.3).

Now, the parameters $\hbar\omega$ and σ_{s0}, having been left as missing data to date, are evaluated by referring to the specimen temperature (see Table 1). The tail spectra of KI at 20 K and 65 K predicted by the Urbach rule thus determined are shown by chain lines in Fig. 1; indeed, the Haupt's 20 K tail is found to be identical to the tail predicted at 77 K. The specimen of the filled circles is certainly on the

		Parameters	Units	F	Cl	Br	I
		σ_{s0}		0.69	0.741	0.765	0.845
		$\hbar\omega$	meV	16.5	9.5	10.7	8.5
	1	A_0	cm^{-1}	$1.0\cdot10^{10}$	$1.2\cdot10^{10}$	$6\cdot10^{9}$	$6\cdot10^{9}$
Na		E_0	eV	10.70	8.025	6.770	5.666
		$2.303\,\frac{\log_{10} A_0}{\sigma_{s0}}$		33.4	31.3	28.8	26.7
	2	$C(1, 10)$	eV	0.163	0.116	0.087	0.058
		$C(1, 10)/\hbar\omega$		9.88	12.2	8.12	6.82
	3	Ref.		9	2	17	17
		σ_{s0}			0.745	0.774	0.830
		$\hbar\omega$	meV		13.5	10.5	4.5
	1	A_0	cm^{-1}		$1.26\cdot10^{10}$	$6\cdot10^{9}$	$6\cdot10^{9}$
		E_0	eV		7.834	6.840	5.890
K		$2.303\,\frac{\log_{10} A_0}{\sigma_{s0}}$			30.8	29.1	27.2
	2	$C(1, 10)$	eV		0.106_8	0.086_5	0.024_5
		$C(1, 10)/\hbar\omega$			7.90	8.24	5.44
	3	Ref.		1			

Table 1. The experimental values of the Urbach-rule parameters for the intrinsic tails in the alkalihalides. $C(\alpha, T) \equiv E_{01}(0) - E(10^{\alpha}, T)$, cf. § 4.

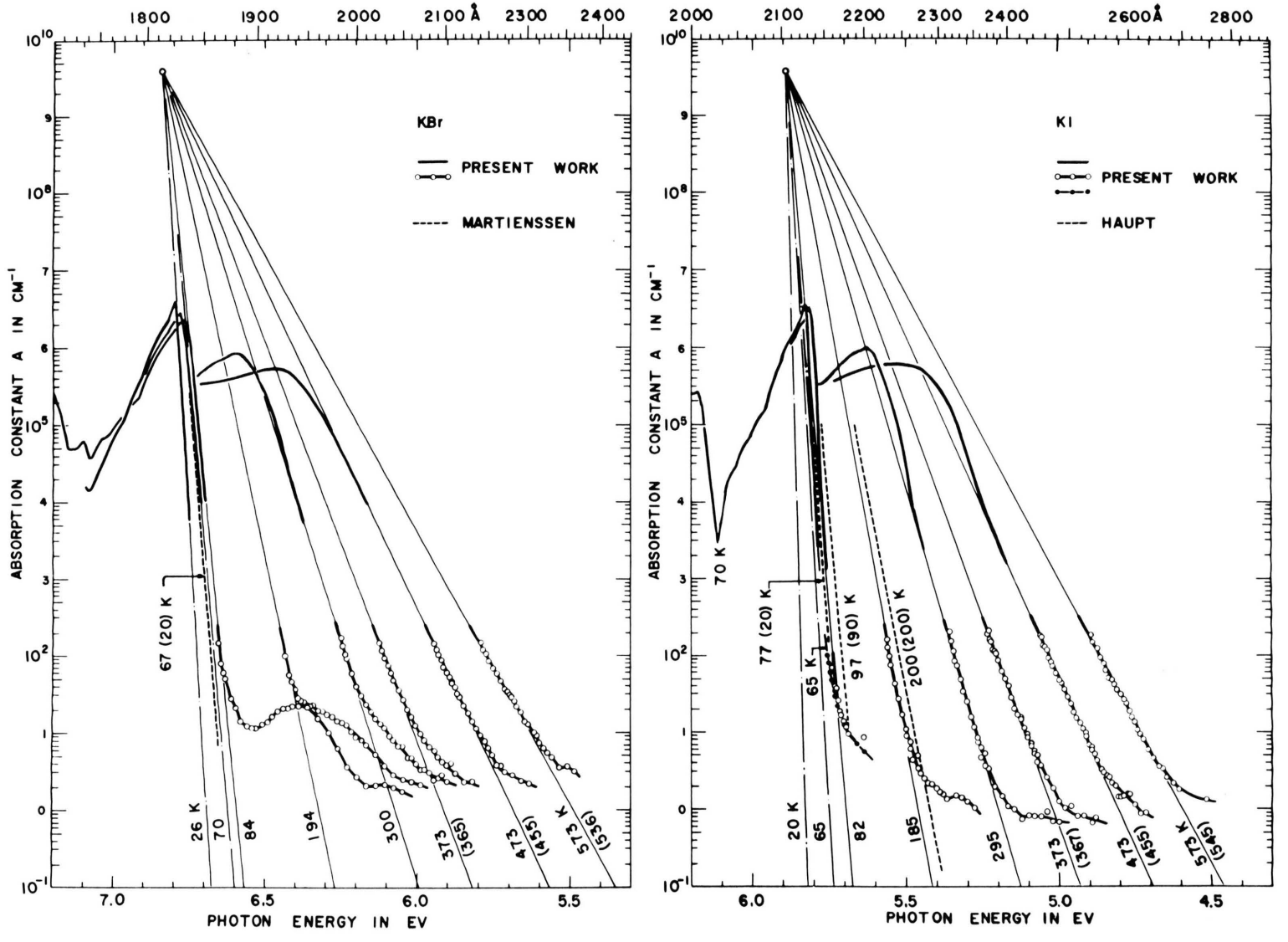

Fig. 1. The spectra of $A(E, T)$ in the lowest energy fundamental region of KBr (left) and KI (right).

lower energy side of the intrinsic tail predicted at 65 K. Similarly, the present Urbach rule for KBr indicates the Martienssen's 20 K-tail at 67 K, see the broken line in Figure 1. It is interesting to note that the above specimen temperature predicted on the "20 K-tail" are nearly equal respectively to the temperature of 69 K estimated by Martienssen as the "Nullpunktstemperatur" of KBr lattice [4] and to the temperature of 66 K ~ 80 K for KI [5]. This suggests it very unlikely that these values have a certain correlation with a lattice dynamical quantity such as a zero-point temperature of lattice. In fact, the zero-point temperature of lattice that the tail can sound is given as $\frac{1}{2}\hbar\omega = 65$ K for KBr and $= 26$ K for KI.

Next we show that the tails below 80 K, the chain lines, are predicted with reasonable accuracy by the present Urbach rule. Generally, the values of $(\hbar\omega, \sigma_{s0})$ derived from the high temperature tails alone do not always locate the tails at their proper positions at lower temperatures (see Fig. 6 in Appendix). However, as detailed in the preceding report [17], whether the tails predicted at low temperatures are correctly located can easily be inferred from the application of the Kramers-Kronig analysis to the reflectivities by observing the non-negativity in the fundamental region and the conformity to the exponential line at its onset region of the converted absorption spectrum. Hence, one can eventually find a pair of values $(\hbar\omega, \sigma_{s0})$ which not only well describe the observed tail spectra at higher temperatures but also yield at lower temperatures the tails compatible with the Kramers-Kronig conversion. Strictly speaking, the values of $(\hbar\omega, \sigma_{s0})$ in Table 1 have been determined in this way except the case of KCl (cf. Appendix), and the chain lines in Fig. 1 have been calculated by the Urbach rule thus determined. The uncertainties in the predicted tail positions are estimated to be within ± 1.5 Å at $A = 10^4\ \mathrm{cm}^{-1}$. On this basis also, it is highly probable that the intrinsic tails at 20 K are *really* located on the higher energy side of the "20 K-tail" in the earlier papers [4, 5].

Figure 2 represents $\sigma_s(T)$ in the sodium- and potassium-halides except KF. Open and filled circles relate to the intrinsic tails actually observed, and the former has been calculated in terms of the specimen-holder temperature and the latter in terms of T_e for $T \gtrsim 370$ K. The double circles stand for $\sigma_s(T)$ of the tails predicted by the Urbach rule in a compatible way with the Kramers-Kronig conversion (the chain lines in Figure 1). The full curve for each halide is calculated by Eq. (2.2) in terms of the specimen temperature making use of $(\hbar\omega, \sigma_{s0})$ in Table 1. The agreement between the calculated and experimental values is fairly good as a whole; especially for chlorides, a closer fit can be achieved between the data and curves over the whole temperature range than the earliers [1, 2]. The behaviour of $\sigma_s(T)$ for NaF is shown by the broken curve, because no intrinsic tails have been observed at any temperature [9].

Now, it is clear from Table 1 that in passing from fluoride to iodide, $\hbar\omega$ becomes smaller and σ_{s0} becomes larger. This tendency of σ_{s0} certainly owes its origin to the constituent halogen ion in these halides, and hence should be explained in terms of a characteristic of the valence band Γ_8^- of each halide as discussed in § 4. Comparing $\hbar\omega$ in Table 1 with the phonon dispersion measurements for each halide [10–13, 19–23], it is found that $\hbar\omega$ in the Urbach rule for the intrinsic tails of the sodium- and potassium-halides has the value nearly equal to the acoustic phonon energy at X or L of each host lattice. Another feature attributable to the halogen ion is noticed on the line shape on the lower energy side of the lowest-energy exciton peak:

In this spectral region, $A(E)$ rises with increasing E first exponentially and subsequently non-exponentially forming the lower energy branch of the asymmetric Lorentzian shape of the main peak. In the case of iodides, the non-exponential part begins around the magnitude range of $A(E)$ as low as a hundredth or less of the peak height and shows a superexponential increase of $A(E)$; owing to this, the lowest-energy exciton peak is located at low temperatures to the lower energy side of the line extrapolating the exponential tail to the convergence point (see Figs. 1 and 3). On the other hand, the non-exponential part of the fluoride and chloride begins subexponentially around the magnitude of $A(E)$ as high as one tenth of the peak height, and hence the peak is always on the higher energy side of the exponential extrapolation line. In the bromides whose σ_{s0} and $\hbar\omega$ are both intermediate among the halides with identical alkali ion, $A(E)$ in the non-exponential part increases with E almost along the extrapolation line.

§ 3. Thermal Shift of the Lowest-Energy Γ-Exciton Peak

This section deals with the apparent peak position ${}^{R}E_{01}(T)$ in the reflectivity spectra (Fig. 4) and the peak $E_{01}(T)$ in the spectra of optical conductivity $\sigma(E)$ (Fig. 5) in the region of the lowest-energy Γ-exciton line; here, $\sigma(E) = n\,K\,E$ in eV and the complex index of refraction $n(E) = n(E) - i\,K(E)$. Open and filled marks in these figures have the same meaning as in Fig. 2, and hence the purpose of this section is to find the best-fit curves for each halide in terms of the specimen temperature T.

Previous works [6, 8, 17, 24] have shown that the lowest-energy Γ-exciton lines $\sigma(E)$ are expressible

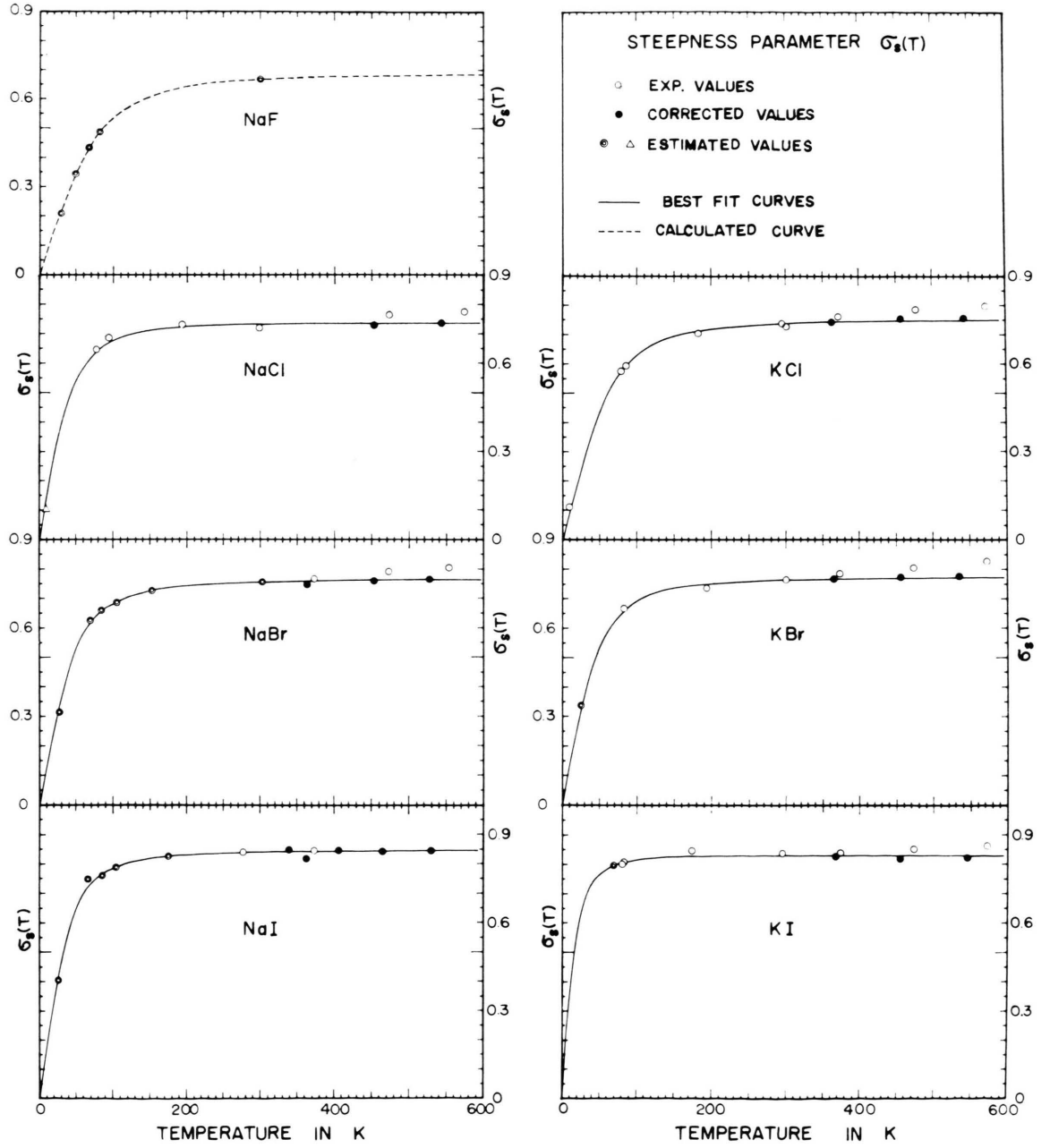

Fig. 2. The data of $\sigma_s(T)$ for the Na- and K-halides except KF; the full and broken curves are calculated by the tanh-law.

in the peak region of the line by the asymmetric Lorentzian function

$$\left.\begin{aligned}\sigma(E) &= \sum_i \frac{\hbar\Gamma_i\sigma_{0i}}{2}\,\frac{\hbar\Gamma_i/2 + 2\Delta_i(E-E_{0i})}{(E-E_{0i})^2+(\hbar\Gamma_i/2)^2}\\ \sigma_{0i} &\equiv \sigma(E_{0i})\end{aligned}\right\}; \quad (3.1)$$

here, suffix $i=1(=2)$ specifies the lower (higher) energy partner of the halogen doublet lines. After the theory [18], one may take this fact as follows: The absorption of photon energy E gives rise to a delocalized exciton whose translational motion is caused by the exciton-phonon interaction. As a result, the half value width $\hbar\Gamma_i$, the degree of asymmetry Δ_i and the peak position E_{0i} are expected to depend on temperature T through $\sum_\omega D(\omega)\big(n(\omega)+(n(\omega)+1)\big)$, where $D(\omega)$ is the phonon distribution function and

$$n(\omega) = [\exp(\hbar\omega/kT)-1]^{-1}$$

is the phonon number. The temperature dependence may be written in a form of $\coth(\hbar\omega/2kT)$ if one describes the phonon field by the Einstein oscillator, regarding $\hbar\omega$ as the effective phonon energy.

As seen in Figs. 4 and 5, the data of ${}^{\mathrm{R}}E_{01}(T)$ and $E_{01}(T)$ are well traced by the full curves calculated respectively by the formulae

$$\begin{aligned}{}^{\mathrm{R}}E_{01}(T) = &\{{}^{\mathrm{R}}E_{01}{}'(0)+{}^{\mathrm{R}}\Delta_1{}'(0)\}\\ &-{}^{\mathrm{R}}\Delta_1{}'(0)\coth(\hbar\omega'/2kT)\,, \end{aligned}\quad (3.2)$$

and

$$\begin{aligned}E_{01}(T) = &\{E_{01}{}'(0)+\Delta_1{}'(0)\}\\ &-\Delta_1{}'(0)\coth(\hbar\omega'/2kT)\,. \end{aligned}\quad (3.3)$$

A list of the parameter-values for the best fit is given in Table 2 for Eq. (3.2) and in column 1 of Table 3 for Equation (3.3). The physical interpretation of the parameters in Eq. (3.3) are difficult to be made because $E_{01}(T)$ involves the contribution $\Delta E_1(T)$ from the thermal dilation of the lattice to the peak shift. Approximating $\Delta E_1(T)$ by the Madelung potential term, Eq. (3.6), one can investigate the contribution of the exciton-phonon interaction to the peak shift $E_{01}(T)-\Delta E_1(T)$:

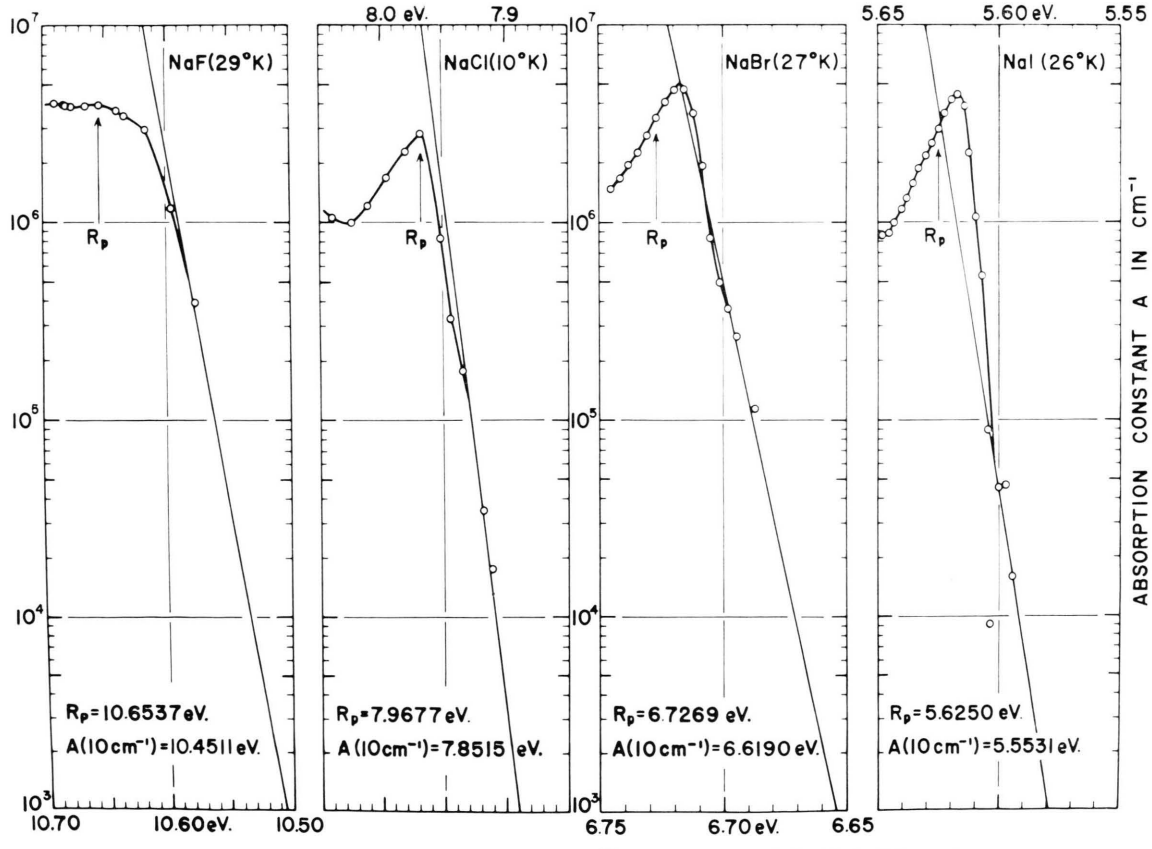

Fig. 3. The entire line shape of $A(E,T)$ in the lowest-energy Γ-exciton region of the Na-halides at low temperatures, where $R_{\mathrm{p}}={}^{\mathrm{R}}E_{01}(T)$.

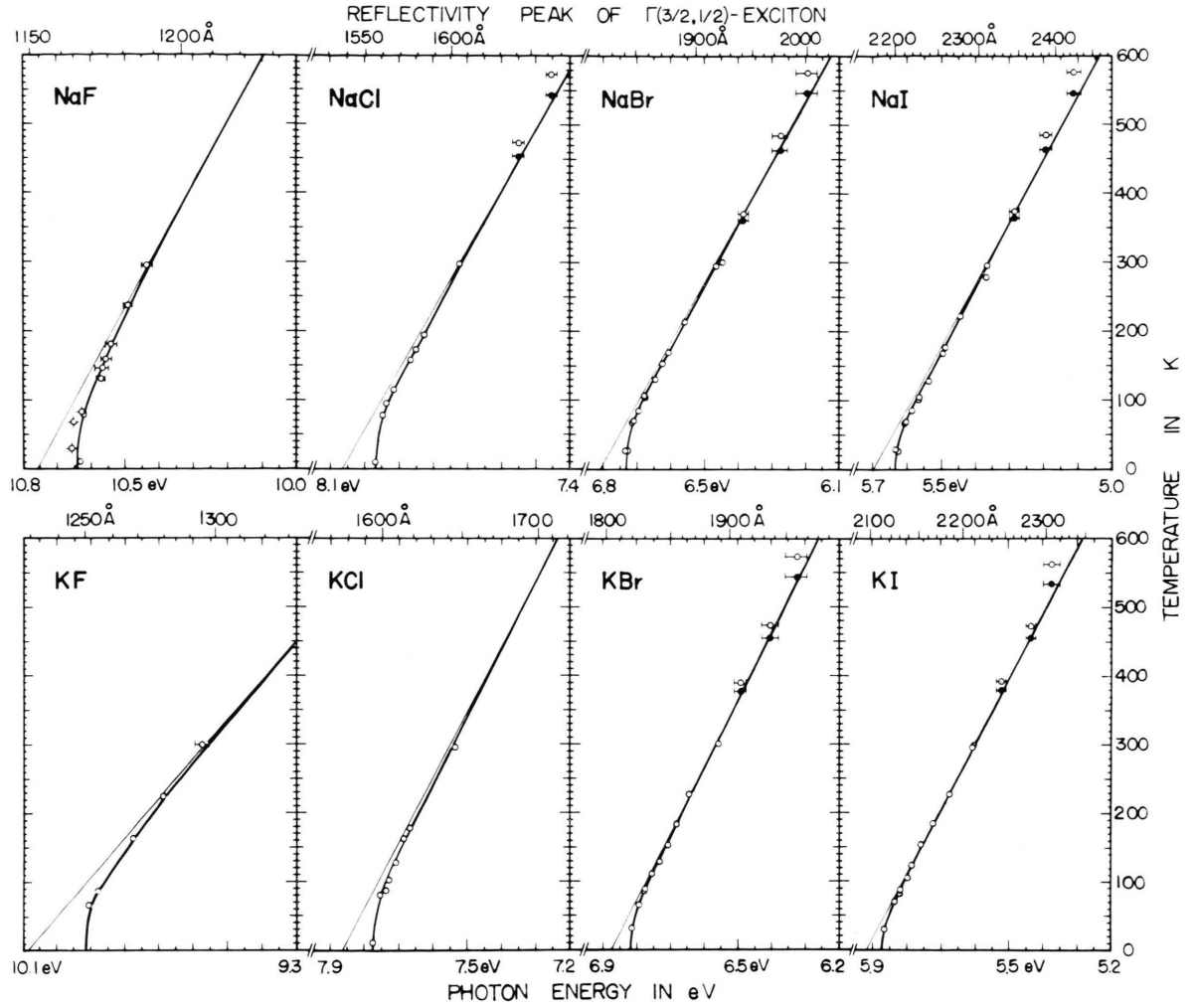

Fig. 4. The data of ${}^{\mathrm{R}}E_{01}(T)$ in the Na- and K-halides; open circles refer to the temperature as measured and filled circles to T_c, and thick solid curves are calculated by the coth-law.

The data of $E_{01}(T) - \Delta E_1(T)$, filled and open triangles in Fig. 5, are traced by the broken curves calculated by

$$E_{01}(T) - \Delta E_1(T) = \{E_{01}(0) + \Delta_1(0)\} - \Delta_1(T) , \tag{3.4}$$

$$\Delta_1(T) \equiv \Delta_1(0) \coth(\hbar\omega/2kT) , \tag{3.5}$$

$$\Delta E_1(T) \equiv -(\alpha_{\mathrm{M}} e^2/\tfrac{1}{2} d_0) \int_0^T \alpha(T)\, \mathrm{d}T . \tag{3.6}$$

Here, the quantities d_0, α_{M} and $\alpha(T)$ are the lattice

	Parameters	Units	F	Cl	Br	I
Na	${}^{\mathrm{R}}E_{01}'(0)$	eV	10.643	7.978	6.730	5.6350
	${}^{\mathrm{R}}\Delta_1'(0)$	eV	0.117	0.095	0.079	0.0599
	${}^{\mathrm{R}}E_{01}'(0) + {}^{\mathrm{R}}\Delta_1'(0)$	eV	10.760	8.063	6.809	5.6949
	$\hbar\omega'$	meV	18.5	14.4	12.0	9.4
K	${}^{\mathrm{R}}E_{01}'(0)$	eV	9.915	7.7763	6.8170	5.8700
	${}^{\mathrm{R}}\Delta_1'(0)$	eV	0.170	0.0860	0.0558	0.0469
	${}^{\mathrm{R}}E_{01}'(0) + {}^{\mathrm{R}}\Delta_1'(0)$	eV	10.085	7.8623	6.8728	5.9169
	$\hbar\omega'$	meV	17.1	14.2	9.5	7.9

Table 2. The temperature dependence of the lowest-energy Γ-exciton peak in the reflectivity spectra of the sodium- and potassium-halides.

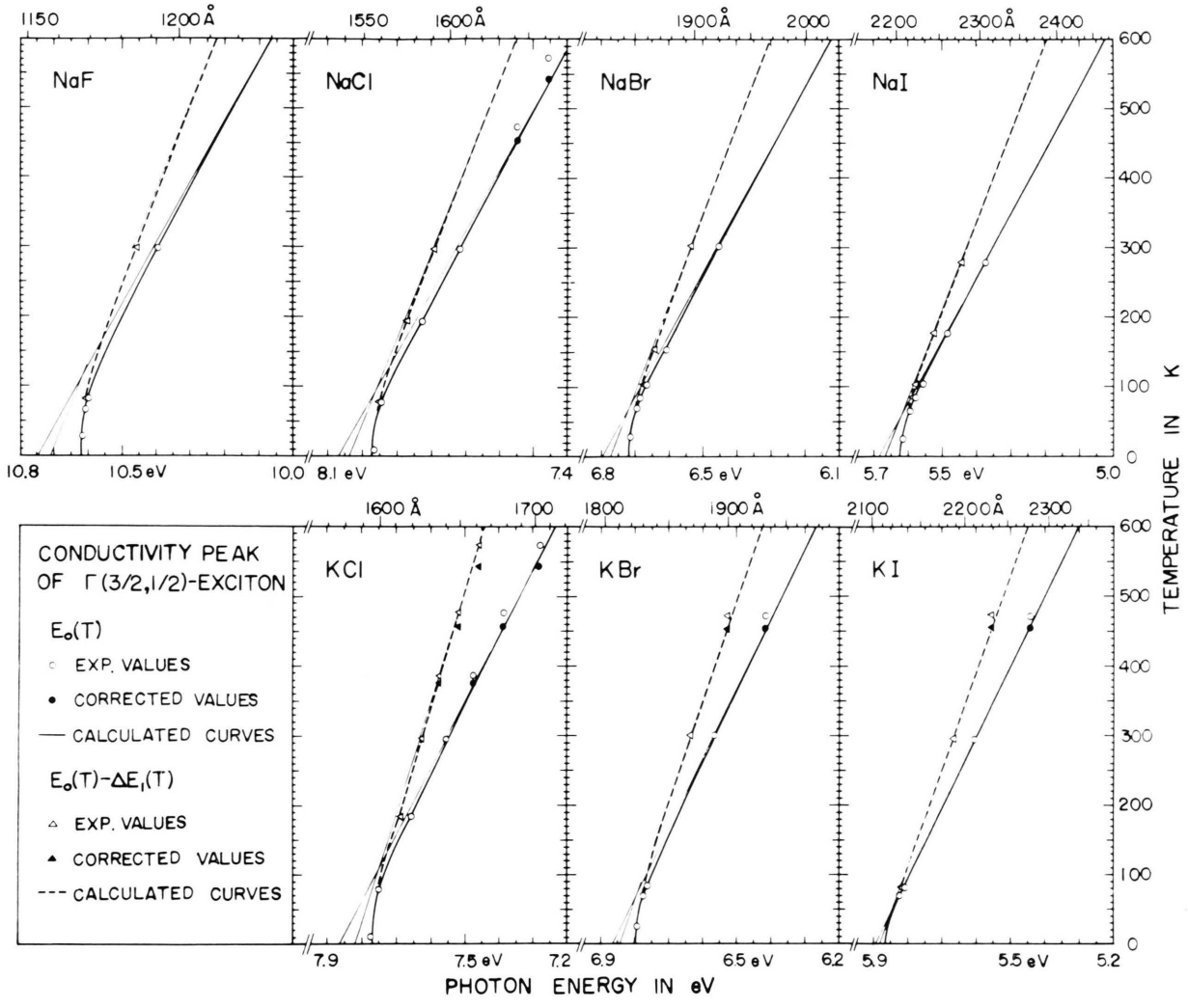

Fig. 5. The data of $E_{01}(T)$ (circles) and $E_{01}(T)-\Delta E_1(T)$ (triangles) of the Na- and K-halides.

constant at $T=0\,\mathrm{K}$, the Madelung constant and the linear coefficient of thermal expansion, respectively. The values of the parameters $E_{01}(0)$, $\Delta_1(0)$ and $\hbar\omega$ for Eq. (3.4) are listed in column 2 of Table 3. The quantity $\Delta_1(T)$ is the self-energy of the $n=1$ state exciton due to the interaction with phonon and $E_{01}(0)+\Delta_1(0)$ corresponds to the purely electronic excitation energy of the $n=1$ state exciton in a *rigid lattice* when $T\to 0\,\mathrm{K}$. This interpretation is conceived to be reasonable because of the formal analogy of the empirical relation (3.4) to the Toyozawa's formula of the peak shift due to the exciton-phonon interaction, viz., Eq. (3.2) in Reference [18].

Denote the quantity relating to the exciton-phonon coupling constant as $W(\omega)$ and its average value as $W_1 \equiv \Sigma_\omega W(\omega) D(\omega) \hbar\omega \{n(\omega)+\frac{1}{2}\} / \Sigma_\omega D(\omega) \hbar\omega \cdot \{n(\omega)+\frac{1}{2}\}$. Then, the energy shift, which is proportional to the numerator of the above fraction, is also well described by the next formula [9]:

$$E_{01}(T) - \Delta E_1(T) = E_{01}(0) - W_1 \int_0^T C_v(T)\,\mathrm{d}T \;; \quad (3.7)$$

here, $C_v(T)$ is the heat capacity at constant volume; a list of the references on $C_v(T)$ and $\alpha(T)$ employed here is given in Table 4. The calculated values are also represented by the broken curves in the figure. In this approximation, each phonon of the possible modes is assumed to interact with the exciton with an equal coupling constant. A list of

Table 3. The temperature dependence of the lowest-energy Γ-exciton peak in the $\sigma(E)$-spectra of the sodium- and potassium-halides.

		Parameters	Units	F	Cl	Br	I
Na	1	$E_{01}'(0)$	eV	10.615	7.968	6.7175	5.6220
		$\Delta_1'(0)$	eV	0.131	0.095	0.0775	0.0605
		$E_{01}'(0)+\Delta_1'(0)$	eV	10.746	8.063	6.7950	5.6825
		$\hbar\omega'$	meV	20	14.4	12	9.6
		$\Delta_1'(0)/\frac{1}{2}\hbar\omega'$		13.1	13.2	12.9	12.6
	2	$E_{01}(0)$	eV	10.615	7.968	6.716	5.622
		$\Delta_1(0)$	eV	0.093	0.065	0.054	0.043
		$E_{01}(0)+\Delta_1(0)$	eV	10.708	8.033	6.770	5.665
		$\hbar\omega$	meV	20	14	12	9.6
		$\Delta_1(0)/\frac{1}{2}\hbar\omega$		9.30	9.28	9.00	8.96
	3	$E_{01}(0)$	eV	10.612	7.9635		5.620
		W_1		1.85	1.68		1.68
	4	$E_g(0)$	eV		8.776	7.165	5.903
K	1	$E_{01}'(0)$	eV		7.7763	6.795	5.8646
		$\Delta_1'(0)$	eV		0.086	0.067	0.0274
		$E_{01}'(0)+\Delta_1'(0)$	eV		7.8623	6.862	5.8920
		$\hbar\omega'$	meV		14.2	11.7	4.81
		$\Delta_1'(0)/\frac{1}{2}\hbar\omega'$			12.1	11.4	11.4
	2	$E_{01}(0)$	eV	9.915	7.7763	6.7955	5.8617
		$\Delta_1(0)$	eV	0.135	0.0400	0.0465	0.0183
		$E_{01}(0)+\Delta_1(0)$	eV	10.050	7.8163	6.8420	5.8800
		$\hbar\omega$	meV	17.1	11	11.7	4.4
		$\Delta_1(0)/\frac{1}{2}\hbar\omega$		15.8	7.28	7.96	8.34
	3	$E_{01}(0)$	eV	9.914	7.7720	6.7950	5.8530
		W_1		2.94	1.46	1.32	1.49
	4	$E_g(0)$	eV	11.384	8.7003	7.529	6.346

the best-fit values of the parameters of Eq. (3.7) is given in column 3 of Table 3.

In a rigid lattice at $T=0$ K, the band-gap energy $E_g^*(0)$ can be written as $\{E_{01}(0)+\Delta_1(0)\}+\{E_{\mathrm{exc},1}+[\Delta_{\mathrm{e,h}}(0)-\Delta_1(0)]\}$, where $E_{\mathrm{exc},1}$ is the binding energy of the lowest-energy exciton in the ground state and $\Delta_{\mathrm{e,h}}(0)$ is the self-energy term of the $n=\infty$ state exciton which is not equal to $\Delta_1(0)$ in general and is not detectable at present by our experiment. However, owing to the presence of the zero-point phonons, the band-gap energy actually observable at the limit of $T\to 0$ K is to be given by

$$E_g(0)=E_{01}(0)+E_{\mathrm{exc},1}\,; \tag{3.8}$$

hence, in column 4 of Table 3 are listed the values of this quantity. Here, the data of $E_{\mathrm{exc},1}$ are quoted from Refs. [6, 8, 17] for KCl, NaCl, NaBr and NaI and also from Ref. [24] for KF, KBr and KI.

Figures 4 and 5 exhibit a very close fit to the data of the calculated curves over the whole temperature range of the experiment in terms of the specimen temperature; in our earlier representation by use of the temperature as measured, any calculated curve failed to fit the data for $T\gtrsim 370$ K. Therefore, the discussion and conclusion on T_c in § 2 are substantiated also by Figs. 2, 4 and 5. The data of KF on the reflectivity peak are missing below 65 K in our experiment (see Figure 4). Our value of 9.915 eV $=E_{01}(0)$ is found to be very close to the recent result on the reflectivity peak 9.87 eV of KF-film at 10 K measured with the slit-width of 0.06 eV at $E=20$ eV [25].

Several features noticeable from the above analyses are as follows:

(1) An empirical relationship

$$E_{01}(0)+\Delta_1(0)\cong E_0 \tag{3.9}$$

holds for KCl, KBr, KI and NaCl in which the intrinsic tails have been evidenced at low temperatures (cf. Tables 1 and 3). The quantity E_0 is defined in Equation (2.1). On this basis, the E_0 was derived for NaF [9], NaBr and NaI [17].

(2) The frequency factors $\hbar\omega'$ and $\hbar\omega$ fall near the point of X or L on the acoustic branches for each host lattice [10–13, 19–23] (cf. Tables 2 and 3).

(3) The inclination of the asymptotic lines against T in Fig. 5 can be given by

$$\frac{\mathrm{d}E_{01}(T)}{\mathrm{d}T}=-k\,\frac{\Delta_1'(0)}{\frac{1}{2}\hbar\omega'}\,, \tag{3.10}$$

$$\frac{\mathrm{d}}{\mathrm{d}T}\{E_{01}(T)-\Delta E_1(T)\}=-k\,\frac{\Delta_1(0)}{\frac{1}{2}\hbar\omega}\,, \tag{3.11}$$

Table 4. A list of the references of the lattice dynamical quantities employed for the analyses of the peak-shift parameters, cf. Eqs. (3.4) and (3.7). $\alpha(T)$: a linear coefficient of thermal expansion; $c_{ij}(T)$: a stiffness parameter; $\chi_S(T)$: a compressibility.

		F	Cl	Br	I
Li	$C_p(T)$	**a**			
	$C_v(T)$	**b**			
Na	$\alpha(T)$	a	b, c, d, e	f, KBr(b)*	d
	$c_{ij}(T)$, $\chi_S(T)$	see, Ref. 9			
	$C_p(T)$	**c**	**a, d**		**e**
	$C_v(T)$	**c**‡	a		**e**
K	$\alpha(T)$	g, NaF(a)*	**a**	b, e, h	d, e, h
	$C_p(T)$	**f**	**e**	**e**	**e**
	$C_v(T)$	**g**	**e**	**e**	**e**

* For example, the notation f, KBr(b)* for NaBr implies that $\alpha(T)$ of NaBr in the whole temperature range is obtained by normalizing $\alpha(T)$ of KBr in Ref. b to $\alpha(T)$ of NaBr in Reference f.

c‡ $C_v(T)$ is converted from $C_p(T)$ given in Ref. **c** by use of the relation

$$C_p(T) - C_v(T) = \frac{C_p(T)}{1 + \{\chi_S(T) \cdot C_p(T)/v\, T \cdot 3^2 \cdot \alpha(T)^2\}},$$

v: the cell volume.

a B. W. James and B. Yates, Phil. Mag. **12**, 253 [1965].
b B. Yates and C. H. Panter, Proc. Phys. Soc. London **80**, 373 [1962].
c G. K. White, Proc. Roy. Soc. London **A 286**, 204 [1965].
d P. P. M. Meincke and G. M. Graham, Canad. J. Phys. **43**, 1853 [1965].
e R. Srinivasan, J. Ind. Inst. Sci. **37**, 232 [1955].
f V. T. Deshpande, Acta Cryst. **14**, 794 [1961].
g R. W. Roberts and C. S. Smith, J. Phys. Chem. Solids **31**, 619 [1970].
h K. E. Salimäki, Ann. Acad. Sci. Fennicae **A VI 56**, 7 [1960].

a Landolt-Börnstein, Zahlenwerte und Funktionen, II. Band, 4. Teil, Springer-Verlag, Berlin 1961.
b B. Yates and C. H. Panter, Proc. Phys. Soc. London **80**, 373 [1969].
c A. J. Kirkham and B. Yates, J. Phys. C **1**, 1162 [1968].
d T. H. K. Barron, A. J. Leadbetter, and J. A. Morrison, Proc. Roy. Soc. London **A 279**, 62 [1963].
e W. T. Berg and Morrison, Proc. Roy. Soc. London **A 242**, 467 [1957].
f E. F. Westrum Jr. and K. S. Pitzer, J. Amer. Chem. Soc. **71**, 1940 [1949].
g $C_v(T)$ is obtained by multiplying $C_p(T)$ in Ref. **f** by the average of $C_v(T)/C_p(T)$ for NaF and LiF.

and their values are listed in Table 3, k being the Boltzmann constant. The quantities W_1 and $\Delta_1(0)/\frac{1}{2}\hbar\omega$ may be used as a measure of the strength of the exciton-phonon coupling (cf. § 4). The quantity $\Delta_1(0)/\frac{1}{2}\hbar\omega$ is seen to depend on the alkali and very little on the halogen; it is ~ 9 for sodium halides and ~ 8 for potassium halides except KF.

§ 4. Discussion

Let us first clarify the concept of the *intrinsic tail* from the phenomenological side and then proceed to the physical considerations on the tail spectra.

It is obvious from the observations hitherto that the empirical relations

$$\left.\begin{array}{l} E_0 \cong E_{01}(0) + \Delta_1(0); \\ A_0 \sim (1.0 \pm 0.5) \cdot 10^{10}\,\mathrm{cm}^{-1}; \\ \hbar\omega \cong \text{acoustic phonon energy at L or X} \end{array}\right\} \quad (4.1)$$

hold for the intrinsic tail spectra *so far as they obey the Urbach rule*. Equations (2.1), (2.2) and (4.1) are conceived to be the best quantitative expression at present for the intrinsic tail spectra of alkalihalides. It is to be noticed that the inclination of the tail against E-axis is *finite* at $T = 0\,\mathrm{K}$, if the tail spectra are to be expressed by the Urbach rule down to this temperature. In this case, the tail position $E(10^0, 0)$, $E(10^\alpha, T)$ being the photon energy of $A = 10^\alpha\,\mathrm{cm}^{-1}$ at T, measured relative to $E_0 \cong E_{01}(0) + \Delta_1(0)$ and scaled by $\frac{1}{2}\hbar\omega$ can be evaluated by use of σ_{s0} and A_0: this is equal to $2.303 \cdot \sigma_{s0}^{-1} \log_{10} A_0$ which is of the order of ~ 33 ~ 27 for the sodium and potassium halides (cf. Table 1). This relation is a revised form of the criterion proposed earlier [Eq. (10b) in Ref. [1]] whose validity is denied by the present results of KBr and KI [cf. $C(\alpha, T)$-values in column 2 of Table 1].

Now, an exponential dependence on E of the tail spectra was displayed in KI by Haupt [5] to the extent as high as $10^5\,\mathrm{cm}^{-1}$. On the other hand, in the present work the exponential line shape in KI is seen in the magnitude range of $A(E,T) \lesssim 10^4\,\mathrm{cm}^{-1}$ at the highest (cf. Fig. 1), and indeed the extent of $A(E,T)$ to which the Urbach rule is applicable varies with the constituent halogen. The difference of the present and Haupt's result is partly due to the use of the Moser-Urbach relation [26], $A(E,T)\,d = 1$, at *low temperatures* in the Haupt's experiment which is allowed only when the validity of exponential law is *a priori* warranted. Accordingly, the earlier experiments [4, 5] are inconsistent in this respect from logical viewpoint. A strict experimental proof was given on the validity of the Urbach rule at low temperatures for KCl however to the extent of $A \lesssim 10^2\,\mathrm{cm}^{-1}$, and this is the sole example to date of the tail spectra amongst the alkalihalides in which the exponential dependence on E is disclosed down to 10 K[1].

A transition of the tail shape occurs in CdTe, as temperature is lowered, from the exponential to non-exponential type in which the phonon structures first appear and then disappear exhibiting a tendency to infinity of the inclination of tail spectrum against E-axis at $T \to 0\,\mathrm{K}$ [27]. In this case, the phonon structures are responsible for the creation of one exciton by the simultaneous annihilation of one photon and one (along with $n \geqq 2$) phonon(s) [28, 29], and hence the exponential tail is nothing but an envelope of the many-phonon sidebands [27]. It is to be noticed that the edge-transition is direct for CdTe, too.

Then, questions naturally arise whether the validity of the Urbach rule is surely kept or whether a transition to CdTe-type is really prohibited in the alkalihalides especially in the iodides on the passage from 10 K to 0 K. These questions ought to be clarified by direct observations in future. The physical significance involved in them has been recently pointed out also from theoretical side by Toyozawa and coworkers in their theory on the Urbach rule [14–16]:

Denote the gain in energy of the free exciton due to the propagation over the undeformed lattice by B and the energy gain of the exciton due to the self-trapping at a lattice site by deforming the surroundings by S. Here, B and S are measured in units of the interacting effective phonon energy. Then, the steepness constant satisfies the relation

$$\sigma_{s0} \cong B/S\,; \tag{4.2}$$

the entire line shape of exciton spectra in the peak- and tail-regions can be explained in terms of the line shape function (3.1) by taking into account the energy dependence, other than the temperature dependence, of the self-energy term $\hat{\Sigma}_1(E,T) = \Delta_1(E,T) - i\hbar\,\Gamma_1(E,T)$. The alkalihalides belong to the regime $B/S<1$ and CdTe-type materials to $B/S>1$.

Now, the halogen dependence of σ_{s0} is discussed. Since B represents the exciton band width scaled with the interacting effective phonon energy, it is inversely proportional to the product of $\hbar\omega$ and the translational effective mass $M = m_h + m_e$ of the exciton at Γ. Our experiment shows that $\hbar\omega$ becomes smaller in going from fluorides to iodides (cf. Tables 1 and 3). Effective hole band-masses m_h as calculated are given by heavy (light) mass = 10.0 (3.2), 6.0 (2.2) and 2.3 (1.7) for KCl [30], KBr [30] and KI [31], respectively; on the other hand, the effective electron band-mass m_e for the potassium salts is of the order of $0.5 \sim 0.3$ [32]. The order of magnitude of S may not so simply be evaluated in alkalihalides. At present, therefore, we can only infer this from W_1 and/or $\Delta_1(0)/\frac{1}{2}\hbar\omega$, both of which exhibit a weak dependence on alkali alone (cf. Table 3). Thus, Eq. (4.2) well explains the observed dependence of σ_{s0} on halogen (cf. Table 1).

Acknowledgements

The present authors would like to thank Professor Y. Toyozawa for many helpful discussions on the exciton-phonon interaction at various stages of this work and for the comments on the original manuscript. They also acknowledge Dr. K. Cho and Dr. H. Sumi for the conversation on their theories. The authors are greatly indebted to Professors T. Shindo and M. Yokoi, the University of Tamagawa, for making the computer facilities available to the authors by sparing their computing time. One of the authors, T. T., acknowledges Professor W. Martienssen, the University of Frankfurt, for the correspondence on the temperature measurements at high temperatures in Ref. [4] and Dr. G. Raunio, the Aktiebolaget Atomenergi in Sweden, for kindly providing a yet unpublished plot of the phonon distribution functions in KCl at 80 K and 300 K at the author's request.

Two of the present authors, T. T. and H. T., dedicate this paper to Professor T. Hibi, the Research Institute for Scientific Measurements of the Tohoku University, on the occasion of celebrating his 63rd birthday.

Appendix

On the Procedure for Obtaining the Best Pair of $(\sigma_{s0}, \hbar\omega)$

This appendix treats a graphical method for finding a pair of $(\sigma_{s0}, \hbar\omega)$ which fits best to observed values $\sigma_s(T_i)$, $i = 1, 2, \ldots, n$, and also treats the definition of the "best". Descriptions are given referring to Figure 6.

Let us suppose n $\sigma_{s0}(T_i, \hbar\omega)$-curves

$$\sigma_{s0}(T_i, \hbar\omega) = (\hbar\omega/2\,k\,T_i)\,\sigma_s(T_i)\cdot\coth(\hbar\omega/2\,k\,T_i)\,; \quad i = 1, 2, \ldots, n \tag{A-1}$$

and n points $\sigma_{s0}(T_i, \hbar\omega_j)$ on these curves crossing with a certain given line $\hbar\omega = \hbar\omega_j$ in the $(\hbar\omega, \sigma_{s0})$-plane. We want to begin with finding the point

$\sigma_{s0}(\hbar\omega_j)$ that makes the deviation

$$\Delta(\hbar\omega_j, \sigma_{s0}(\hbar\omega_j)) \equiv \Sigma_i \{\sigma_s(T_i) - \sigma_s(T_i, \hbar\omega_j)_{cal}\}^2 \tag{A-2}$$

minimum, where

$$\sigma_s(T_i, \hbar\omega_j)_{cal} = \sigma_{s0}(\hbar\omega_j)\, n_{ij}^{1/2};$$
$$n_{ij}^{1/2} \equiv \sigma_s(T_i)/\sigma_{s0}(T_i, \hbar\omega_j)\ .$$

Differentiating Eq. (A-2) with respect to $\sigma_{s0}(\hbar\omega_j)$ and setting the derivative equal to zero, $\sigma_{s0}(\hbar\omega_j)$ is given by

$$\sigma_{s0}(\hbar\omega_j) = \Sigma_i n_{ij} \cdot \sigma_{s0}(T_i, \hbar\omega_j)/\Sigma_i n_{ij}\ . \tag{A-3}$$

Substituting this into Eq. (A-2), the minimum deviation $\Delta_{min}(\hbar\omega_j)$ at $\hbar\omega = \hbar\omega_j$ is given by

$$\Delta_{min}(\hbar\omega_j) = \Sigma_i \sigma_s(T_i)^2 \cdot \left\{1 - \sigma_{s0}(T_i, \hbar\omega_j)^{-1}\ \frac{\Sigma_i n_{ij} \cdot \sigma_{s0}(T_i, \hbar\omega_j)}{\Sigma_i n_{ij}}\right\}^2 . \tag{A-4}$$

Numerical computations of the quantities $\sigma_{s0}(\hbar\omega_j)$ and $\Delta_{min}(\hbar\omega_j)$ are easily performed, because $\sigma_s(T_i)$ is experimentally known and $\sigma_{s0}(T_i, \hbar\omega_j)$ can be evaluated graphically. The value of $\hbar\omega = \hbar\omega^*$ that makes $\Delta_{min}(\hbar\omega_j)$ minimum against a variation of $\hbar\omega_j$ and $\sigma_{s0}{}^* = \sigma_{s0}(\hbar\omega^*)$ constitute a pair for the best fit to the observed values of $\sigma_s(T_i)$. The definition of the "best" fit in this case is expressed by

$$\Delta_{min} = \Sigma_i \{\sigma_s(T_i) - \sigma_s(T_i)_{cal}\}^2, \tag{A-5}$$

where

$$\sigma_s(T_i)_{cal} = \sigma_{s0}{}^* \frac{2kT}{\hbar\omega^*} \tanh \frac{\hbar\omega^*}{2kT}\ .$$

In the text, a pair for the best fit is simply denoted as $(\sigma_{s0}, \hbar\omega)$. Equation (A-3) clearly indicates that the most probable point $\sigma_{s0}(\hbar\omega_j)$ at $\hbar\omega_j$ is not evaluated by

$$\Sigma_i \sigma_{s0}(T_i, \hbar\omega_j)/n \tag{A-6}$$

because of a weight n_{ij} at each cross point.

We can also evaluate a pair of parameters under a separate definition of the best fit, e. g., by making the deviation

$$\Delta'(\hbar\omega_j) \equiv \Sigma_i \left\{\frac{\sigma_s(T_i) - \sigma_s(T_i, \hbar\omega_j)_{cal}}{\sigma_s(T_i)}\right\}^2 = \Sigma_i \left\{1 - \frac{\sigma_{s0}(\hbar\omega_j)}{\sigma_{s0}(T_i, \hbar\omega_j)}\right\}^2 \tag{A-7}$$

minimum. In this case we have

$$\sigma_{s0}(\hbar\omega_j) = \Sigma_i n_{ij}' \cdot \sigma_{s0}(T_i, \hbar\omega_j)/\Sigma_i n_{ij}',$$
$$n_{ij}' \equiv \sigma_{s0}(T_i, \hbar\omega_j)^{-2}, \tag{A-8}$$

and

$$\Delta'_{min}(\hbar\omega_j) = \Sigma_i n_{ij}' \{\sigma_{s0}(T_i, \hbar\omega_j) - \sigma_{s0}(\hbar\omega_j)\}^2 . \tag{A-9}$$

A comparison:

(A-5) → $\sigma_{s0} = 0.754$; $\hbar\omega = 13.5$ meV,
(A-6) → $\sigma_{s0} = 0.749 \pm 0.018$; $\hbar\omega = 13.5$ meV $\pm$ 1.8 meV,
(A-9) → $\sigma_{s0} = 0.745$; $\hbar\omega = 12.0$ meV,
} for KCl

where the best point given by (A-5) is shown by the open circle in Figure 6.

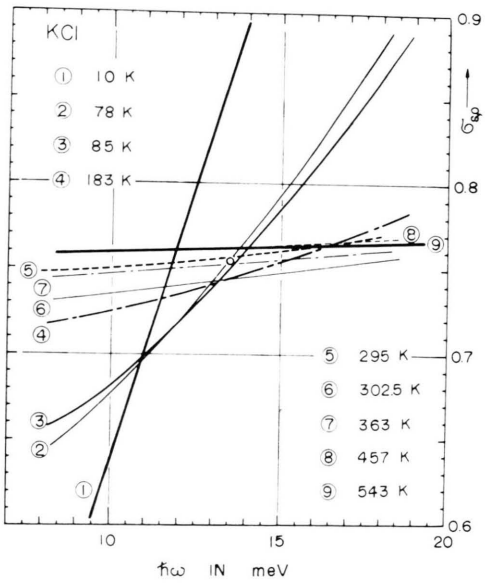

Fig. 6. The $\sigma_{s0}(T, \hbar\omega)$-curves of KCl at various temperatures represented as a function of $\hbar\omega$; the open circle represents the best set of values of $(\sigma_{s0}, \hbar\omega)$ derived from Equation (A-5).

[1] T. Tomiki, J. Phys. Soc. Japan **23**, 1280 [1967].
[2] T. Miyata and T. Tomiki, J. Phys. Soc. Japan **22**, 209 [1967].
[3] H. Mahr, Phys. Rev. **125**, 1510 [1962].
[4] W. Martienssen, J. Phys. Chem. Solids **2**, 257 [1957].
[5] U. Haupt, Z. Phys. **157**, 232 [1959].
[6] T. Tomiki, J. Phys. Soc. Japan **22**, 463 [1967].
[7] T. Tomiki, J. Phys. Soc. Japan **26**, 738 [1969].
[8] T. Miyata and T. Tomiki, J. Phys. Soc. Japan **24**, 1286 [1968].
[9] R. Sano, J. Phys. Soc. Japan **27**, 695 [1969].
[10] J. R. D. Copley, R. W. MacPherson, and T. Timusk, Phys. Rev. **182**, 965 [1969].
[11] G. Raunio and L. Almqvist, Phys. Stat. Sol. **33**, 209 [1969].
[12] G. Raunio, L. Almqvist and R. Stedman, Phys. Rev. **178**, 1496 [1969].
[13] R. E. Schmunk and D. R. Winder, J. Phys. Chem. Solids **31**, 131 [1970].

[14] Y. Toyozawa, Proc. 10th International Conf. on Phys. of Semiconductors, Cambridge, Mass. 1970 (published by the United States Atomic Energy Commission, 1970) p. 5.
[15] K. Cho and Y. Toyozawa, J. Phys. Soc. Japan **30**, 1555 [1971].
[16] H. Sumi and Y. Toyozawa, J. Phys. Soc. Japan **31**, 342 [1971].
[17] T. Miyata, J. Phys. Soc. Japan **31**, 529 [1971].
[18] Y. Toyozawa, Progr. Theor. Phys. Supplmt. No. 12, 111 [1960].
[19] A. D. B. Woods, B. N. Brockhouse, R. A. Cowley, and W. Cochran, Phys. Rev. **131**, 1025 [1963].
[20] G. Dolling, R. A. Cowley, C. Schittenhelm, and I. M. Thorson, Phys. Rev. **147**, 577 [1966].
[21] W. J. L. Buyers, Phys. Rev. **153**, 923 [1967].
[22] W. Bührer, Phys. Stat. Sol. **41**, 789 [1970].
[23] J. S. Reid, T. Smith, and W. J. L. Buyers, Phys. Rev. **B 1**. 1833 [1970].
[24] T. Tomiki, T. Miyata, and H. Tsukamoto, J. Phys. Soc. Japan **35**, 495 [1973].
[25] D. Blechschmidt, R. Haensel, E. E. Koch, U. Nielsen, and M. Skibowski, Phys. Stat. Sol. **44**, 787 [1971].
[26] F. Moser and F. Urbach, Phys. Rev. **102**, 1519 [1956].
[27] D. T. F. Marple, Phys. Rev. **150**, 728 [1966].
[28] B. Segall, Phys. Rev. **150**, 734 [1966].
[29] D. G. Thomas, J. J. Hopfield, and M. Power, Phys. Rev. **119**, 570 [1960].
[30] H. Overhof, Phys. Stat. Sol. (b), **43**, 575 [1971].
[31] Y. Onodera, J. Phys. Soc. Japan **25**, 469 [1968]. — Y. Onodera, M. Okazaki, and T. Inui, J. Phys. Soc. Japan **21**, 2229 [1966].
[32] J. W. Hodby, J. Phys. C (Solid State Phys.) **4**, L8 [1971].